Resonance Raman Spectroscopic Characterization of the π-Anion and π-Cation Radicals of Zinc(II) Octaethylchlorin

Milton E. Blackwood, Jr., and Thomas G. Spiro*

Department of Chemistry, Princeton University, Princeton, New Jersey 08544

Received: April 17, 1997; In Final Form: June 24, 1997[⊗]

Cyclic voltammetry (CV), UV−vis spectroscopy, and resonance Raman (RR) spectroscopy are utilized to characterize the π-anion and π-cation radicals of ZnOEC (OEC = octaethylchlorin). Features in the RR spectra are assigned with the aid of data from the *meso*−d_4 isotopomer of ZnOEC and ZnEtI (EtI = etiochlorin I). The vibrational frequency shift patterns of the radicals are consistent with expected bonding changes on placing an electron in the LUMO or a hole in the HOMO. The frontier orbitals are similar in ZnOEC and ZnOEP (OEP = octaethylporphyrin), but the anion spectra differ because of the consequences of the Jahn−Teller effect in $ZnOEP^-$. The cation and anion vibrational shifts do not add to give the shifts previously reported for the triplet state, indicating additional distortion upon triplet excitation.

Introduction

The π-radicals of metallochlorins are of wide interest because of their roles in photosynthetic light harvesting, energy transfer, and electron transfer.[1] Metallochlorins differ from metalloporphyrins in that they contain a reduced pyrrole ring. This ring reduction has significant effects on the ground state structural[2] and electronic[3] properties of metallochlorins as compared to their parent metalloporphyrins, but the consequences for the radical species are less well understood. Resonance Raman (RR) spectroscopy has been used extensively to characterize the π-radicals of metalloporphyrins.[4−10] Similar studies of metallochlorins are beginning to allow comparisons to be made between the physical properties of π-radicals of metallochlorins and metalloporphyrins.

RR spectra for the π-cations of Zn(II), Cu(II), Co(II), and Ni(II) complexes of methyloctaethylchlorin (MeOEC) have been reported.[11] In addition, Perng and Bocian have used RR spectroscopy to examine the π-anion of Zn(OEC) (OEC = octaethylchlorin).[12] In neither study was isotopic labeling used to assign the Raman features. We have recently investigated the anion of Zn(II) tetraphenylchlorin, ZnTPC, and several of its isotopomers[13] and have also used time-resolved RR spectroscopy in conjunction with isotope labeling to characterize the first triplet, T_1, excited states of ZnTPC[14] and ZnOEC.[15]

In the present study, we use RR spectroscopy to characterize the π-anion and π-cation species of ZnOEC (Figure 1). Naturally occurring metallochlorins are β-substituted, and it is important to determine how this substitution pattern affects the properties of the radicals. We have also studied the *meso*-d_4 isotopomer of ZnOEC as well as Zn(II) etiochlorin, ZnEtI (Figure 1), permitting assignment of the vibrational modes. These data and those previously published for ZnOEP (OEP = octaethylporphyrin) are interpreted in terms of the expected changes in electronic structures.

Experimental Section

Materials. Free-base octaethylchlorin, H_2OEC, and etiochlorin I, H_2EtI, were prepared from Fe(III) octaethylporphyrin·Cl and Fe(III) etioporphyrin I·Cl (Midcentury Chemicals), respectively, according to Whitlock et al.[16] The *meso*−hydrogens of H_2OEC were exchanged by stirring natural abundance (NA) H_2OEC in D_2SO_4/D_2O overnight. Zinc(II) was inserted into the free-base NA H_2OEC and H_2EtI by refluxing with Zn(II) acetate in dimethylformamide (DMF). For the *meso*-d_4 free base, the metal insertion was performed by refluxing with $ZnCl_2$ in a chloroform/CH_3OD solution to prevent back exchange of *meso* hydrogens. All compounds were purified on 1000 μm alumina chromatograph plates using a hexane/THF eluant (60%/40% v:v).

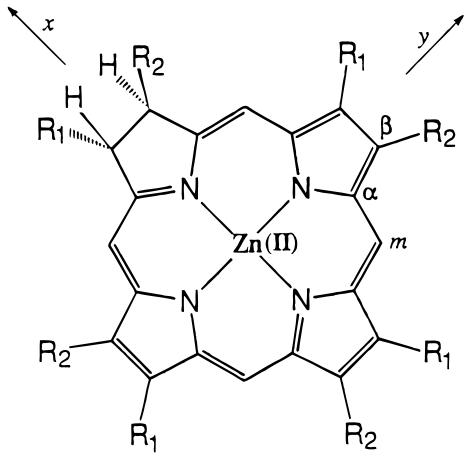

ZnOEC: $R_1 = R_2 = C_2H_5$

ZnEtI: $R_1 = CH_3$

$R_2 = C_2H_5$

Figure 1. Molecular structures and labeling scheme for Zn(II) octaethylchlorin (ZnOEC) and Zn(II) etiochlorin I (ZnEtI).

Tetrahydrofuran (THF) was distilled in the presence of sodium and benzophenone, and methylene chloride (CH_2Cl_2) was distilled in the presence of calcium hydride. Both solvents were deoxygenated by four freeze−pump−thaw cycles and transferred to a glovebox equipped with a dri-train prior to use. Tetrabutylammonium perchlorate (TBAP) (recrystallized from ethanol and dried in a vacuum oven at 90 °C overnight) at ∼0.2 M served as the supporting electrolyte in all electrochemical experiments.

Electrochemistry and Spectroelectrochemistry of ZnOEC and ZnEtI. A Princeton Applied Research Model 173 potentiostat was used to control the potential in all experiments. Cyclic voltammetry was performed with a standard three-electrode cell

[⊗] Abstract published in *Advance ACS Abstracts,* September 1, 1997.

S1089-5647(97)01351-5 CCC: $14.00

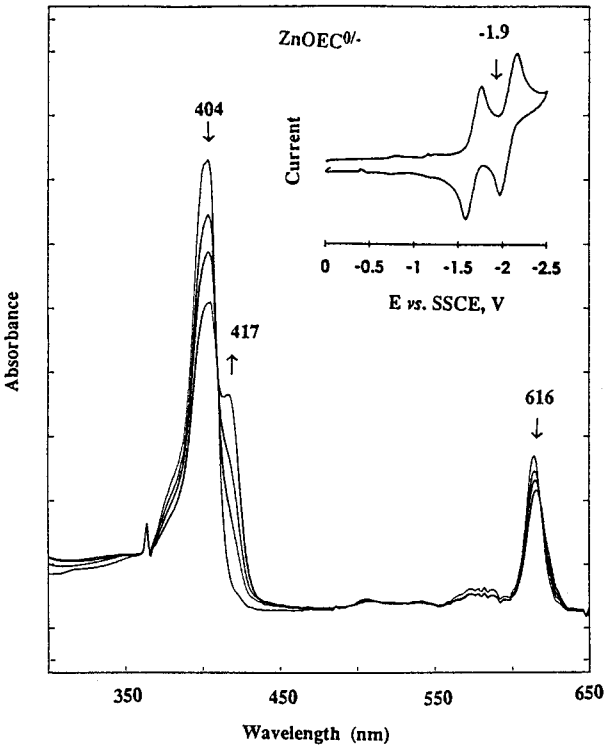

Figure 2. Electronic absorption spectra of ZnOEC and its radical anion in THF. The anion was generated by electrolysis of the neutral parent at −1.9 V. Arrows indicate the direction of change with increasing degree of electrolysis. The inset shows the cyclic voltammogram of ZnOEC (in THF, 100 mV/s scan rate) scanned from 0 to −2.5 V.

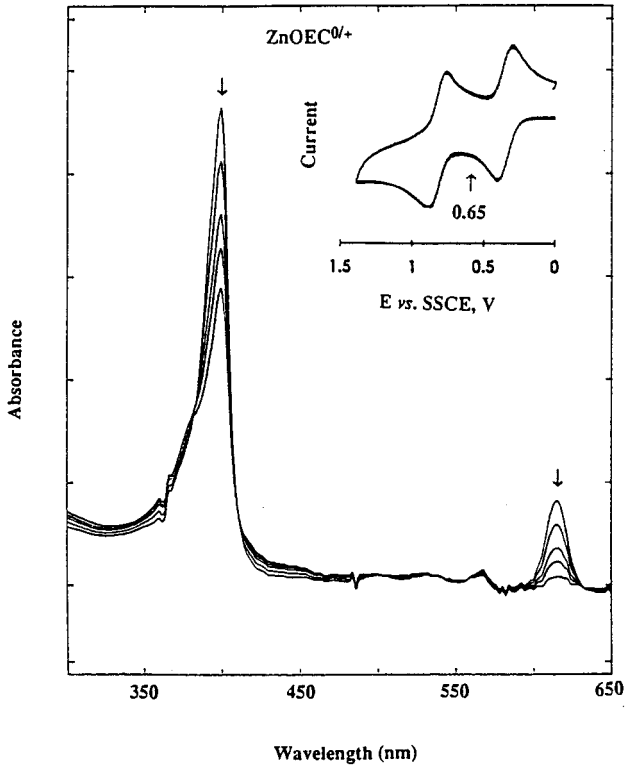

Figure 3. Electronic absorption spectra of ZnOEC and its radical cation in CH_2Cl_2. The cation was generated by electrolysis of the neutral parent at 0.65 V. The inset show the cyclic voltammogram of ZnOEC (in CH_2Cl_2, 100 mV/s scan rate) scanned from 0 to 1.5 V.

with a polished platinum working electrode. The bulk electrolysis cell for the measurement of Raman spectra[17] and the optically transparent thin-layer electrochemical (OTTLE) cell for the measurement of the UV−vis spectra[18] have been described previously. All electrochemical cells were assembled in a glovebox equipped with a dri-train. The electronic spectra were obtained on a Hewlett-Packard 8452A diode array spectrometer.

Resonance Raman Spectroscopy. RR spectra were obtained via 135° backscattering geometry with continuous stirring to minimize photodamage. Excitation lines were provided from a Kr^+ laser (413 nm) and an Ar^+ laser (365 nm). The scattered light was dispersed with a single-stage spectrograph and detected with a liquid N_2 cooled CCD (Princeton Instruments). The laser powers at the sample were approximately 15 mW, and spectral acquisition times were 10 min. After measuring each radical RR spectrum, the neutral parent spectrum was regenerated electrochemically to ensure that decomposition had not occurred. Sample integrity also was checked by UV−vis absorption spectroscopy after each experiment. All data were processed with Labcalc software (Galactic Industries Corp.).

Results

Electronic Absorption Spectra of the ZnOEC Cation and Anion Radicals. Figure 2 shows the UV−vis absorption spectrum of the ZnOEC anion generated by electrolysis of the neutral parent at −1.9 V. This potential is slightly more negative than the first reversible reduction potential of ZnOEC in THF (see cyclic voltammogram in the inset). Direct conversion to the anion without byproduct contamination is confirmed by the appearance of isosbestic points at 370, 410, and 552 nm. The neutral parent spectrum could be regenerated quantitatively when the anion was oxidized at 0.0 V. Reduction produces a shoulder (417 nm) on the low-energy side of the Soret band region and weakens the Q_y absorption band (616 nm). The ZnOEC anion spectrum differs from that obtained by Perng and Bocian,[12] who reported an 8-fold intensity decrease and a slight shift of the Soret band along with the appearance of several new features in the longer wavelength region. It is unclear whether the different solvent (butyronitrile) and supporting electrolyte (tetrabutylammonium hexafluorophosphate) used in their study could account for the differences. Our $ZnOEC^-$ absorption spectrum more closely resembles those reported previously for metalloporphyrin[5,7,19] and metallochlorin[13] anions.

The absorption spectrum for the cation of ZnOEC in CH_2Cl_2 is shown in Figure 3. Electrolysis was carried out at +0.65 V, slightly more positive than the first oxidation wave of the cyclic voltammogram (Figure 3, inset). Oxidation of ZnOEC results in bleaching of the Q-bands and diminished intensity together with a slight blue-shift in the Soret band. The spectrum is similar to the ZnOEP (OEP = octaethylporphyrin) radical cation spectrum.[20] Clear isosbestic points are seen in the oxidative electrolysis of ZnOEC (at 380, 410, and 600 nm), and the neutral parent could be regenerated quantitatively when the radical cation was reduced at 0.0 V.

Neutral Resonance Raman Spectra. The RR spectra of ZnOEC, its *meso*-d_4 isotopomer, and ZnEtI in THF (413 nm excitation) and in CH_2Cl_2 (365 nm excitation) are shown in Figures 4 and 5, respectively. Different solvents were utilized because the ZnOEC anion was found to be stable in THF, while the cation was stable in CH_2Cl_2. Assignments are based upon previous RR studies and normal mode analyses of β-substituted metallochlorins[11,12,15,21] and metalloporphyrins,[22] with peak labeling based on the parent metalloporphyrin modes, as worked out for NiOEC.[23] The high-frequency stretching modes are at slightly lower frequencies in THF than in CH_2Cl_2, because THF coordinates the Zn(II) and expands the chlorin core.[24] The 413 nm excited spectrum has been reported previously,[15] but several

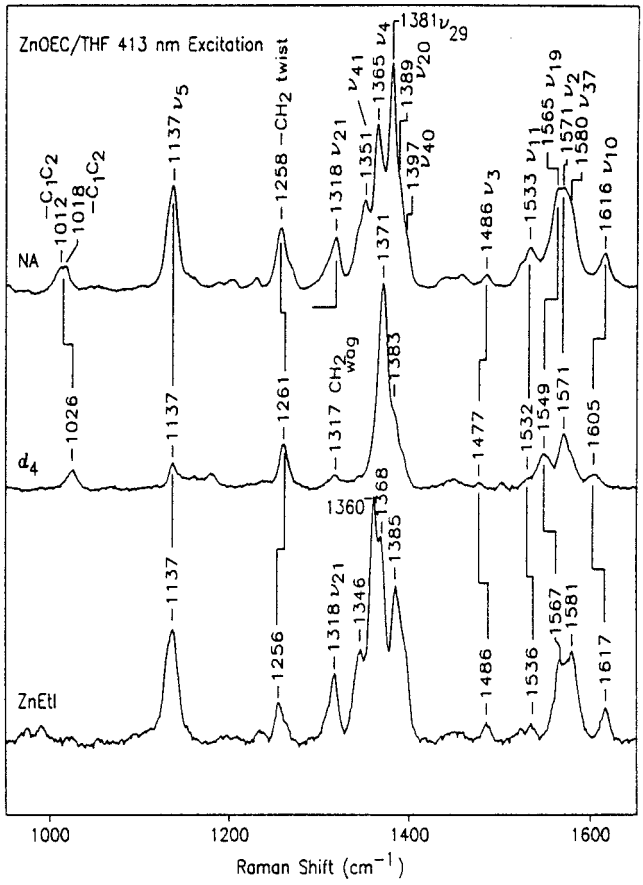

Figure 4. The 413 nm excited RR spectra of natural abundance (NA) ZnOEC, the *meso*-d_4 isotopomer of ZnOEC, and ZnEtI in THF.

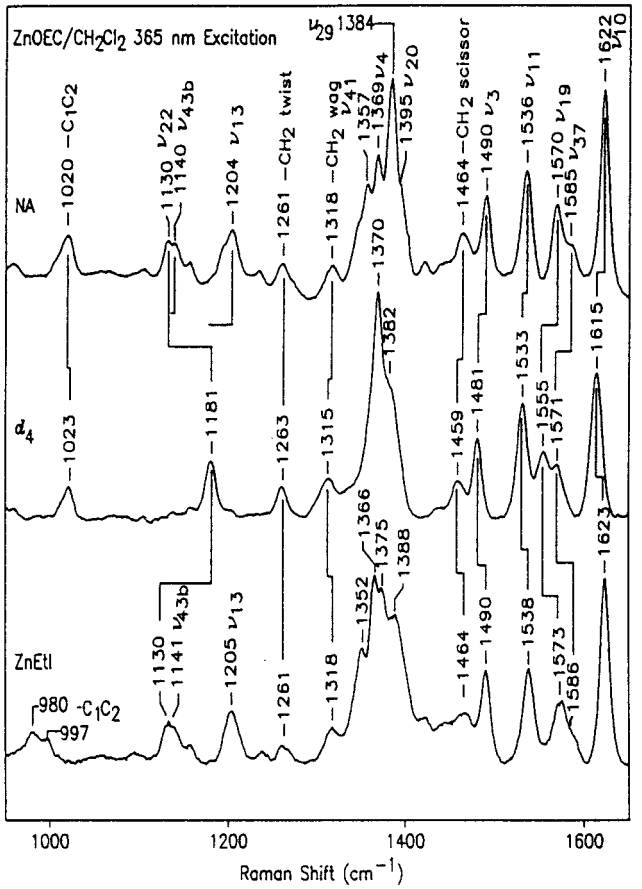

Figure 5. The 365 nm excited RR spectra of natural abundance (NA) ZnOEC, the *meso*-d_4 isotopomer of ZnOEC, and ZnEtI in CH_2Cl_2.

new bands are enhanced with 365 nm excitation and are assigned to the skeletal modes ν_{22} (1130 cm^{-1}), ν_{43b} (1140 cm^{-1}), and ν_{13} (1204 cm^{-1}) and the substituent modes $-CH_2$ wagging (1318 cm^{-1}) and $-CH_2$ scissoring (1464 cm^{-1}) based on their isotope shifts.[22,23] Vibrational assignments are summarized in Table 1.

Radical Anion and Cation Resonance Raman Spectra. The RR spectra of the ZnOEC and ZnEtI radical anions (in THF) and cations (in CH_2Cl_2) are shown in Figures 6 and 7, respectively. Bands are correlated with features in the spectra of the neutral species on the basis of similar isotope and substituent shifts (Table 2).

In the neutral chlorin, two $C_\beta C_\beta$ stretching modes, ν_2 and ν_{11}, are identified via their insensitivity to *meso* deuteration and their slight upshifts in ZnEtI, which has a lower effective C_β substituent mass, but these modes are not detected in the radical anion. All the high-frequency anion bands are *meso*-d_4 sensitive and are assigned to $C_\alpha C_m$ stretching modes. Two of these, ν_{19} and ν_{37}, shift down strongly (-23 and -16 cm^{-1}) while the other two, ν_2 and ν_{10}, shift up slightly ($+2$ and $+3$ cm^{-1}). In the 1320$-$1400 cm^{-1} region of the spectrum, where peaks due to $C_\alpha N$ and $C_\alpha C_\beta$ stretching modes are dominant, vibrational frequency downshifts of a few cm^{-1} are observed, while a lower frequency $C_\alpha C_\beta$ stretching mode, ν_5, shifts up ($+5$ cm^{-1}) in ZnOEC$^-$. No significant frequency shifts are observed for the substituent modes. A new feature at 1134 cm^{-1} does not clearly correlate with any ground-state peak and remains unassigned.

Perng and Bocian[12] reported a quite different RR spectrum for ZnOEC$^-$, one which differs very little from the neutral parent. We believe this spectrum actually does arise largely from the neutral parent, which experiences strong resonance enhancement at the selected excitation wavelength, 406.7 nm. In our experience 406.7 nm excited spectra always contained remnant features from trace quantities of the neutral parent. Only by switching to 413 nm, which is closer to resonance with the 417 nm absorption band of ZnOEC$^-$ (Figure 2), were we able to obtain clean RR spectra of the anion radical.

In the cation radical RR spectrum, two $C_\beta C_\beta$ stretches (1590 and 1603 cm^{-1}) are again identified by *meso*-d_4 insensitivity and upshifts in ZnEtI$^+$. One of these is assigned to ν_2 and the other to ν_{38}, the frequency being too high for ν_{11}.[23] ν_{38} is not observed in neutral ZnOEC, but ν_2 is seen to shift up fully 32 cm^{-1} in the cation. Three $C_\alpha C_m$ stretching modes are identified for the radical cation. Two of these, ν_3 and ν_{19}, shift in the same direction and by a similar amount ($+3$ and -29 cm^{-1}) as in the radical anion, but the third, ν_{10}, shifts down (-10 cm^{-1}) instead of up. In the 1300$-$1400 cm^{-1} region of the spectrum overlapping of Raman peaks arising from $C_\alpha C_\beta$ and $C_\alpha N$ stretching modes[23] makes definitive assignments difficult, but all the bands are shifted down by -12 to -15 cm^{-1}. Two substituent modes observed in the cation, the C_1C_2 stretching mode (1021 cm^{-1}) and the $-CH_2$ twist (1261 cm^{-1}), are not significantly shifted from their neutral vibrational frequencies. A new feature in the cation spectrum at 1234 cm^{-1} is assigned to ν_{42b}, primarily a hydrogen bending mode in NiOEC.[23] Several weak features in the 1100$-$1200 cm^{-1} region of the cation spectrum do not correlate well with any NiOEP or NiOEC modes and, thus, remain unassigned.

The cation RR spectrum is consistent with that reported by Salehi et al.[11] for Zn(MeOEC)$^+$, which did not, however, have the benefit of isotope assignments. The two assignments that were made, ν_3 and ν_{10} (on the basis of frequency shifts upon metal substitution), are in agreement with ours.

TABLE 1: Ground-State Vibrational Frequencies (cm^{-1}) for Natural Abundance (NA) ZnOEC, *meso*-d_4 ZnOEC, and ZnEtI[a]

mode	NA in THF	Δd_4[b]	ΔZnEtI[c]	NA in CH_2Cl_2	Δd_4[b]	ΔZnEtI[c]
$\nu_{10}(C_\alpha C_m$	1616	−11	+1	1622	−7	+1
$\nu_{37}(C_\alpha C_m$	1580	*	+1	1585	−14	+1
$\nu_{38}(C_\beta C_\beta)$	*	*	*	*	*	*
$\nu_2(C_\beta C_\beta)$	1571	0	*	*	*	*
$\nu_{19}(C_\alpha C_m)$	1565	−16	+2	1570	−15	+3
$\nu_{11}(C_\beta C_\beta)$	1533	−1	+3	1536	−3	+2
$\nu_3(\alpha C_m)$	1486	−9	0	1490	−9	0
$-CH_2$ scissor	*	*	*	1464	−5	0
$\nu_{40}(C_\alpha N, C_\alpha C_\beta)$	1397	*	*	*	*	*
$\nu_{20}(C_\alpha N, C_\alpha C_\beta)$	1389	*	*	1395	*	*
$\nu_{29}(C_\alpha N, C_\alpha C_\beta)$	1381	*	*	1384	*	*
$\nu_4(\alpha N, C_\alpha C_\beta)$	1365	*	*	1369	*	*
$\nu_{41}(C_\alpha N, C_\alpha C_\beta)$	1351	*	*	1357	*	*
$-CH_2$ wag	*	(1317)	*	1318	−3	0
$\nu_{21}(\delta CCH, \delta C_m H)$	1318	*	0	*	*	*
$-CH_2$ twist	1258	+3	−2	1261	+2	0
$\nu_{42b}(\delta C_m H, \delta CCH)$	*	*	*	*		*
$\nu_{13}(\delta C_m H, C_\alpha C_\beta)$	*	*	*	1204	*	+1
$\nu_{43b}(C_\alpha N, \delta C_\alpha C_m H)$	*	*	*	1140	*	+1
$\nu_{22}(C_\alpha N, C\beta C_1, \delta C_\alpha C_m H)$	*	*	*	1130	+51	0
$\nu_5(C_\alpha C_\beta, C_\beta H)$	1137	0	0	*	*	*
$-C_1C_2$	1018	+6	(991)[c]	1020	+3	(997)[d]
$-C_1C_2$	1012	*	*	*	*	(980)[d]

[a] Asterisks indicate unobserved or not assignable. [b] Frequency shift upon *meso*-d_4 substitution. [c] Frequency shift between ZnOEC and ZnEtI. [d] Mode composition for $-C_1C_2$ is likely different between ZnOEC and ZnEtI because of the differing substituent patterns in the two molecules.

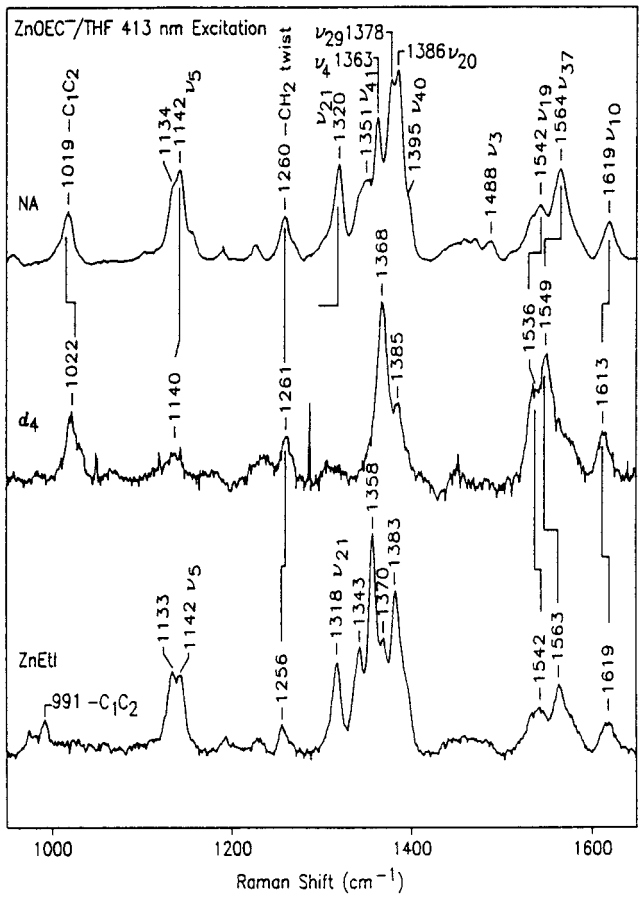

Figure 6. The 413 nm excited RR spectra of the π-anions of natural abundance (NA) ZnOEC, the *meso*-d_4 isotopomer of ZnOEC, and ZnEtI in THF.

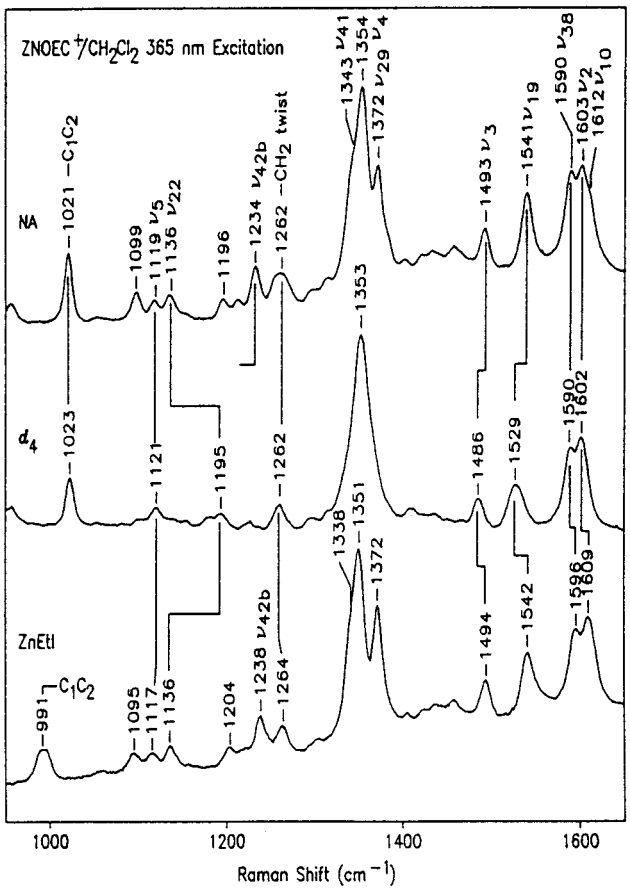

Figure 7. The 365 nm excited RR spectra of the π-cations of natural abundance (NA) ZnOEC, the *meso*-d_4 isotopomer of ZnOEC, and ZnEtI in CH_2Cl_2.

Discussion

The mode frequency shifts upon ZnOEC cation and anion formation can be interpreted in terms of bonding changes upon extracting an electron from the HOMO or adding and electron to the LUMO (Figure 8).[25] The orbital patterns are much the same as those of the octaethylporphyrin (OEP) frontier orbitals (Figure 8),[25] despite the reduction of one of the $C_\beta C_\beta$ double bonds in chlorin.

Cation Radical. In OEP, the HOMO is the a_{1u} orbital, whose energy is elevated above the a_{2u} orbital by the electron-donating properties of the C_β ethyl substituents and the concentration of a_{1u} electron density on the C_β atoms.[26] In contrast, the a_{2u} electron density is concentrated on the C_m atoms, and the a_{2u}

TABLE 2: Vibrational Frequencies (cm^{-1}) for ZnOEC and Its π-Anion and π-Cation Radicals[a]

mode	ZnOEC(THF)	$ZnOEC^-$	$\Delta^{-/0}$ [b]	$ZnOEC(CH_2Cl_2)$	$ZnOEC^+$	$\Delta^{+/0}$ [c]
ν_{10}	1616	1619	+3	1622	1612	−10
ν_{37}	1580	1564	−16	1585	*	
ν_{38}	*	*		*	1590	
ν_2	1571	*		*	1603	
ν_{19}	1565	1542	−23	1570	1541	−29
ν_{11}	1533	*		1536	*	
ν_3	1486	+2	1490	1493	+3	
$-CH_2$ scissor	*	*		1464	*	
ν_{40}	1397	1395	−2	*	*	
ν_{20}	1389	1386	−3	1395	*	
ν_{29}	1381	1378	−3	1384	1372	−12
ν_4	1365	1363	−3	1369	1354	−15
ν_{41}	1351	1351	0	1357	1343	−14
$-CH_2$ wag	*	*		1318	*	*
ν_{21}	1318	1320	+2	*	*	
$-CH_2$ twist	1258	1260	+2	1261	1262	+1
ν_{42b}	*	*		*	1234	
ν_{13}	*	*		1204	*	
ν_{14}	*	*		1140	*	
ν_5	1137	1142	+5	*	1119	
ν_{22}	*	*		1130	1136	+6
C_1C_2	1018	1019	+1	1020	1021	+1
C_1C_2	1012	*		*	*	

[a] Asterisks indicate unobserved or not assignable. [b] Frequency shift upon anion radical formation. [c] Frequency shift upon cation radical formation.

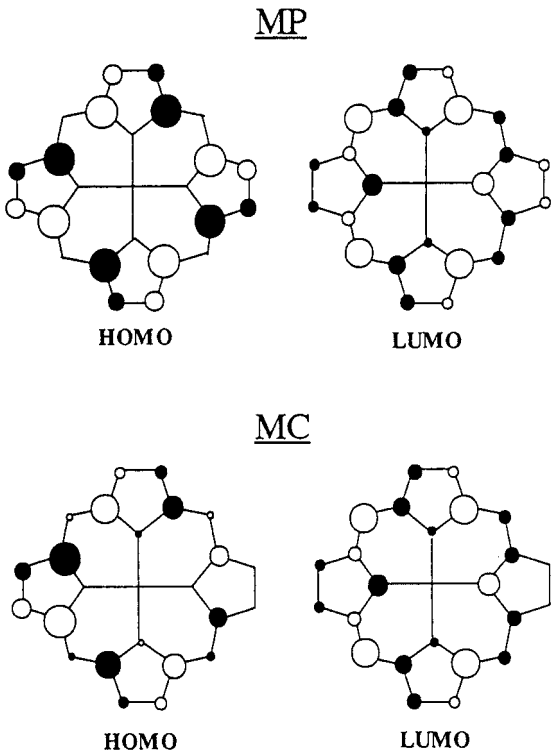

Figure 8. Illustrations of the HOMOs and LUMOs for a metalloporphyrin (MP) and a metallochlorin (MC) adapted from ref 25. Only the a_{1u} orbital is shown for the HOMO of metalloporphyrins.

energy is raised above the a_{1u} energy in the *meso*-substituted tetraphenylporphyrins (TPP's).[26] In chlorins, reduction of one of the $C_\beta C_\beta$ double bonds further raises the energy of the orbital deriving from the a_{1u} porphyrin orbital. Consequently, the HOMO bond pattern is similar in OEP and OEC. In both cases, extraction of an electron is expected to strengthen the $C_\beta C_\beta$ bonds, because of the a_{1u} antibonding character, and to weaken the $C_\alpha C_\beta$ bonds, because of the a_{1u} bonding character. These expectations are met in both $ZnOEP^+$ and $ZnOEC^+$. The $C_\beta C_\beta$ stretches ν_2 and ν_{11} are elevated (+19 and +28 cm^{-1}) in $ZnOEP^+$, and the $C_\alpha C_\beta/C_\alpha N$ stretch ν_4 is lowered (−34 cm^{-1}).[20] Likewise, ν_2 is raised (+32 cm^{-1}) in $ZnOEC^+$ (ν_{11} is not detected) and ν_4 is lowered (−15 cm^{-1}), as are the nearby $C_\alpha C_\beta/C_\alpha N$ modes ν_{29} (−12 cm^{-1}) and ν_{41}(−14 cm^{-1}).

However, the OEP and OEC HOMO's differ slightly with respect to the $C_\alpha C_m$ bonds. The OEP a_{1u} orbital has nodes at the C_m atoms, and little change in the $C_\alpha C_m$ bonds is expected upon oxidation. Indeed, the shifts of the $C_\alpha C_m$ stretches, ν_{10} and ν_3, are small (−1 and −8 cm^{-1}) in $ZnOEP^+$.[20] The ZnOEC HOMO does have electron density at the C_m atoms, however (Figure 8), reflecting some mixing of a_{2u} character, which is allowed in the lowered symmetry of the chlorin. The orbital is alternately bonding and antibonding with respect to the $C_\alpha C_m$ bonds. This explains the observed downshifts in the ν_{10} and ν_{19} modes (−10 and −29 cm^{-1}), both of which are out-of-phase with respect to the adjacent $C_\alpha C_m$ bonds,[23] and the concerted expansion and contraction of these bonds reinforces the HOMO orbital pattern. In contrast, ν_3, which involves in-phase stretching of adjacent $C_\alpha C_m$ bonds,[23] is shifted very little.

Anion Radical. Analysis of the anion radical pattern is complicated by the fact that, although the LUMO's of ZnOEP and ZnOEC are again very similar (Figure 8), the porphyrin has two degenerate LUMO's and is subject to a Jahn−Teller (J−T) distortion,[27] while reduction of the $C_\beta C_\beta$ bond leads to a nondegenerate LUMO for the chlorin. The J−T distortion has been shown to involve a B_{1g} symmetry expansion and contraction of opposite sides of the ring and amplifies the bonding pattern of the LUMO.[7] Thus, the out-of-phase $C_\alpha C_m$ stretches ν_{19}, ν_{37}, and ν_{10} are lowered moderately, on average, in $ZnOEC^-$ (−23, −16, and +3 cm^{-1}), reflecting the alternate $C_\alpha C_m$ bonding and antibonding character of the LUMO (see analogous effect in the HOMO, above), but ν_{10} shifts down strongly (−26 cm^{-1}) in $ZnOEP^-$ (the other modes are not detected).[7]

In $ZnOEP^-$, the A_{1g} symmetry $C_\beta C_\beta$ stretch, ν_2, shifts only slightly (−12 cm^{-1}) reflecting the alternate $C_\beta C_\beta$ bonding and antibonding character of the e_g* orbitals, while the B_{1g} symmetry $C_\beta C_\beta$ stretch ν_{11} shifts down very strongly (−52 cm^{-1}), as a result of the superimposed J−T effect.[7] In $ZnOEC^-$, the $C_\beta C_\beta$ modes have not been identified and are apparently not resonance enhanced.

Finally, the $C_\alpha C_\beta/C_\alpha N$ modes ν_{29} and ν_4 shift only slightly (−3 and −3 cm^{-1}) in $ZnOEC^-$, reflecting the cancellation of bonding and antibonding contributions on either side of two

TABLE 3: Comparison of Selected Vibrational Frequency Shifts (cm^{-1}) in the Anion, Cation, and T_1 State of ZnOEC[a]

mode	$\Delta^{-/0}$	$\Delta^{+/0}$	$\Delta(T_1-S_0)$[b]
ν_{10}	+3	−10	−19
ν_{37}	−16	*	*
ν_2	*	+32[c]	−29
ν_{19}	−23	−29	*
ν_3	+2	+3	−22
ν_{20}	−2	*	*
ν_{29}	−3	−12	−7
ν_4	−3	−15	−21
ν_{41}	0	−14	*

[a] Asterisks indicate not assignable. [b] From ref 15. [c] Frequency shift determined from ground-state value measured in a different solvent (THF) than was the cation (CH_2Cl_2).

out of three pyrrole rings (Figure 8), while in $ZnOEP^-$ ν_4 shift down by 2 cm^{-1} and ν_{29} by 13 cm^{-1}.[7] The ZnOEP LUMO is antibonding for both $C_\alpha C_\beta$ and $C_\alpha N$ on two of the four pyrrole rings. Moreover, ν_{29} is a B_{2g} symmetry mode and can participate in the J−T distortion (although the B_{2g} contribution to the distortion is minor).[7]

Triplet State. RR spectra and assignments for the T_1 state of ZnOEC are reported elsewhere,[15] and it is of interest to compare the excited-state shifts with the radical anion and cation shifts. Since the T_1 electronic excitation involves transfer of an electron from the HOMO to the LUMO, the accompanying structural effects might be expected to be additive. However, the sums of the anion and cation frequency shifts are far from those observed in the triplet state (Table 3). For example, neither the in-phase nor the out-of-phase $C_\alpha C_m$ stretches, ν_3 and ν_{10}, are particularly sensitive to cation or anion formation, yet both shift down strongly in the T_1 state (−22 and −19 cm^{-1}), indicating a decrease in average $C_\alpha C_m$ bond order. Also, the $C_\beta C_\beta$ stretch ν_2 shifts down strongly upon triplet formation but shifts up on cation formation; it has not been detected in the anion, but there is no reason to expect a large shift.

A similar lack of additivity was earlier noted for ZnOEP and tentatively ascribed to the differing effects of J−T distortions in the anion and triplet species.[7,8,20,28] However, there is no J−T distortion for the ZnOEC anion or triplet. Moreover, the cation and anion shifts have also been found to be nonadditive for the triplet state of free-base tetraphenylbacteriochlorin (two reduced $C_\beta C_\beta$ bonds), in which there is again no Jahn−Teller effect.[28] For all three tetrapyrrole macrocycles, the pattern of frequency shifts upon radical cation and anion formation are explicable on the basis of the bonding pattern of the HOMO and LUMO, at least qualitatively. However, this is not true for any of the triplet states. These results indicate additional distortion upon triplet excitation. The source of this effect is uncertain and is a challenge to theory, since at the level of MNDO/3 calculations, the predicted geometry changes in the triplet state of Zn porphine were found to be approximately the sum of the changes in the radical cation and anion.[29]

Acknowledgment. This work was supported by NIH Grant GM 33576.

References and Notes

(1) (a) Frew, J. E.; Jones, P. *Adv. Inorg. Bioinorg. Mech*. **1984**, *3*, 175−212. (b) Mathies, R.; Rutherford, A. W. in *Photosynthesis*; Amesz, J., Ed.; Elsevier: Amsterdam, 1987; pp 63−96. (c) Scheer, H., Ed. *Chlorophylls*; CRC: Boca Raton, FL, 1991. (d) DiMagno, T. J.; Wang, Z.; Norris, J. R. *Curr. Opinion Struct. Biol.* **1992**, *2*, 836−842.

(2) (a) Spaulding, L. D.; Andrews, L. C.; Williams, G. J. B. *J. Am. Chem. Soc*. **1977**, *99*, 6918−6923. (b) Strauss, S. H.; Silver, M. E.; Ibers, J. A. *J. Am. Chem. Soc*. **1983**, *105*, 4108−4109.

(3) Gouterman, M. Physical Chemistry, Part A. In *The Porphyrins*, Dolphin, D., Ed.; Academic Press: New York, 1978; Vol. III.

(4) Procyk, A. D.; Bocian, D. F. *Annu. Rev. Phys. Chem*. **1992**, *43*, 465−496.

(5) Lin, C.-Y.; Spiro, T. G. *Inorg. Chem*. **1996**, *35*, 5237−5243.

(6) Kumble, R.; Loppnow, G. R.; Hu, S.; Mukherjee, A.; Thompson, M. A.; Spiro, T. G. *J. Phys. Chem*. **1995**, *99*, 5809−5816.

(7) Hu, S.; Lin, C.−Y.; Blackwood, Jr., M. E.; Mukherjee, A.; Spiro, T. G. *J. Phys. Chem*. **1995**, *99*, 9694−9701.

(8) Kreszowski, D. H.; Deinum, G.; Babcock, G. T. *J. Am. Chem. Soc*. **1994**, *116*, 7463−7464.

(9) Perng, J. H.; Bocian, D. F. *J. Phys. Chem*. **1992**, *93*, 4804−4811.

(10) Kumble, R.; Hu, S.; Loppnow, G. R.; Vitols, S. E.; Spiro, T. G. *J. Phys. Chem*. **1993**, *97*, 10521−10523.

(11) Salehi, A.; Oertling, W. A.; Fonda, F. N.; Babcock, G. T.; Chang, C. K. *Photochem. Photobiol*. **1988**, *48*, 525−530.

(12) Perng, J.; Bocian, D. F. *J. Phys. Chem*. **1992**, *96*, 10234−10240.

(13) Blackwood, M. E., Jr.; Lin, C.−Y.; Cleary, S. R.; McGlashen, M. L.; Spiro, T. G. *J. Phys. Chem. A* **1997**, *101*, 255−258.

(14) Vitols, S. E.; Terashita, S.; Blackwood, M. E., Jr.; Kumble, R.; Spiro, T. G. *J. Phys. Chem.* **1995**, *99*, 7246−7250.

(15) Blackwood, Jr., M. E.; Kumble, R.; Spiro, T. G. *J. Phys. Chem*. **1996**, *100*, 18037−18041.

(16) Whitlock, H. W., Jr.; Hanauser, R.; Oester, M. Y.; Bower, B. K. *J. Am. Chem. Soc.* **1976**, *41*, 3857−3860.

(17) Czernuszewicz, R. S.; Macor, K. A. *J. Raman Spectrosc*. **1988**, *19*, 553.

(18) Lin, C.-Y.; McGlashen, M. L.; Hu, S.; Shim, Y. K.; Smith, K. M.; Spiro, T. G. *Inorg. Chim. Acta* **1996**, *252*, 179−184.

(19) Reed, R. A.; Purello, R.; Prendergast, K.; Spiro, T. G. *J. Phys. Chem*. **1991**, *95*, 9720−9727.

(20) Oertling, W. A.; Salehi, A.; Chung, Y. C.; Leroi, G. E.; Chang, C. K.; Babcock, G. T. *J. Phys. Chem.* **1987**, *91*, 5887−5898

(21) (a) Ozaki, Y.; Kitagawa T.; Ogoshi, H. *Inorg. Chem*. **1979**, *18*, 1772−1776. (b) Ozaki, Y.; Iriyama, H.; Ogoshi, H.; Ochiai, T.; Kitagawa, T. *J. Phys. Chem.* **1986**, *90*, 6105−6112, 6113−6118. (c) Boldt, N. J.; Donohoe, R. J.; Birge, R. R.; Bocian, D. F. *J. Am. Chem. Soc*. **1987**, *109*, 2284−2298. (d) Salehi, A.; Oertling, W. A.; Fonda, F. N.; Babcock, G. T.; Chang, C. K. *Photochem. Photobiol.* **1988**, *48*, 525−530. (e) Procyk, A. D.; Kim, Y.; Schmidt, E.; Fonda, H. N.; Chang, C. K.; Babcock, G. T.; Bocian D. F. *J. Am. Chem. Soc*. **1992**, *114*, 6539−6549.

(22) Li, X.-Y.; Czernuszewicz, R. S.; Kincaid, J. R.; Stein, P.; Spiro, T. G. *J. Phys. Chem*. **1990**, *94*, 47−61.

(23) Prendergast, K.; Spiro, T. G. *J. Phys. Chem.* **1991**, *95*, 1555−1563.

(24) Prendergast, K.; Spiro, T. G. *J. Am. Chem. Soc*. **1992**, *114*, 3793−3801.

(25) Sekino, H.; Kobayashi H. *J. Chem. Phys*. **1987**, *86*, 5045−5052.

(26) Czernuszewicz, R. S.; Macor, K. A.; Li, X.-Y.; Kincaid, J. R.; Spiro, T. G. *J. Am. Chem. Soc*. **1989**, *111*, 3860−3869.

(27) Hoffman, B. M.; Ratner, M. A. *Mol. Phys*. **1978**, *35*, 901−925.

(28) Lin, C.-Y.; Blackwood, M. E., Jr.; Kumble, R.; Hu, S.; Spiro, T. G. *J. Phys. Chem. B* **1997**, *101*, 2372−2380.

(29) Prendergast, K.; Spiro, T. G. *J. Am. Chem. Soc*. **1991**, *95*, 9728−9736.